Sensitivity of Atmospheric Motion Vectors Height Assignment Methods to Semitransparent Cloud Properties Using Simulated Meteosat-8 Radiances

Régis Borde, Philippe Dubuisson

Sensitivity of Atmospheric Motion Vectors Height Assignment Methods to Semitransparent Cloud Properties Using Simulated *Meteosat-8* Radiances

RÉGIS BORDE

EUMETSAT, Darmstadt, Germany

PHILIPPE DUBUISSON

Laboratoire d'Optique Atmosphérique, Lille, France

(Manuscript received 23 July 2009, in final form 15 January 2010)

ABSTRACT

This paper presents the sensitivity to various atmospheric parameters of two height assignment methods that aim to retrieve the cloud-top height of semitransparent clouds. The use of simulated *Meteosat-8* radiances has the advantage that the pressure retrieved by a given method can be compared to the initial pressure set to the cloud in the model, which is exactly known. The methods retrieve the pressure of a perfectly opaque cloud to within a few hectopascals. However, considering more realistic ice clouds, methods are sensitive to all of the tested atmospheric parameters and, especially, to the cloud microphysics, which can bias the results of the CO_2-slicing method by several tens of hectopascals. The cloud-top pressure retrieval is especially difficult for thinner clouds with optical thicknesses smaller than 2, for which the errors can reach several tens of hectopascals. The methods have also been tested after introducing realistic perturbations in the temperature and humidity profiles and on the clear-sky surface radiances. The corresponding averages of errors on the retrieved pressures are also very large, especially for thin clouds. In multilayer cloud situations the height assignment methods do not work properly, placing the cloud-top height somewhere between the two cloud layers for most cirrus cloud layers with optical thicknesses between 0.1 and 10.

1. Introduction

Atmospheric motion vectors (AMVs) are one of the most important products derived from geostationary satellites and constitute a significant part of the observational data fed to numerical weather prediction (NWP) models. Indeed, they provide wind observations with good coverage for the tropics and midlatitudes, especially over the large ocean areas. The European Organisation for the Exploitation of Meteorological Satellites (EUMETSAT) wind vectors are extracted from the visible channel at 0.8 μm (VIS0.8) and the infrared (IR) channel at 10.8 μm (IR10.8) by tracking clouds in consecutive Meteosat Second Generation (MSG) images (Schmetz et al. 2002), and from water vapor (WV) channels centered at 6.2 μm (WV6.2) and at 7.3 μm (WV7.3) by tracking water vapor features. Low-level AMVs are also extracted from the high-resolution visible channel. The final hourly AMV product disseminated by EUMETSAT is an average of three vectors calculated from a sequence of four MSG images.

The basic elements of wind vector production at EUMETSAT (Holmlund 2000) are (a) selecting a feature to track, (b) tracking the target in a time sequence of images to obtain a relative motion, (c) assigning a pressure (altitude) to the vector, and (d) assessing the quality of the vector. The height assignment (HA) step, which estimates the cloud-top height in the case of cloud motion vectors, is still recognized to be the largest source of error in this AMV extraction process (Forsythe and Doutriaux-Boucher 2005). Problems with height assignment are especially frequent at high levels, in strong wind shear situations, and can have a negative impact on the forecast from NWP models when such AMVs are assimilated by the models.

The algorithm used to set the height of the AMVs at EUMETSAT is quite complicated, as it uses different methods depending on the type of target tracked. For opaque clouds the measured window channel IR10.8 brightness temperature is matched against a collocated

Corresponding author address: Régis Borde, EUMETSAT, EUMETSAT Allee 1, D-64295 Darmstadt, Germany.
E-mail: regis.borde@eumetsat.int

DOI: 10.1175/2010JAMC2352.1

temperature profile obtained from forecast data of the NWP model, which is assumed to be accurate. Specific methods are applied for low-level AMVs, setting the wind altitude to the level of the temperature inversion when it exists, or to the cloud base (Le Marshall et al. 1993). It is beyond the aim of this paper to describe in detail all of these techniques. The most important problem occurs for semitransparent clouds, for which part of the signal received by the satellite is composed of the contribution of the surface and/or cloudy layers below. In these cases, the brightness temperature technique used for opaque clouds cannot be applied as the retrieved pressure would be too low in the troposphere. Several techniques exist to correct the estimation of the cloud-top pressure for this semitransparency effect (Szejwach 1982; Nieman et al. 1993; Schmetz et al. 1993; Smith and Platt 1978; Menzel et al. 1983; Eyre and Menzel 1989). Relative to Meteosat's first generation, the multichannel imagery of MSG provides new opportunities for the height assignment of semitransparent clouds. The presence of the CO_2 channel at 13.4 μm allows for the use of the CO_2-slicing method, in addition to the former H_2O-intercept method (referred to as STC in the following) used at EUMETSAT since the first generation of Meteosat satellites (Szejwach 1982; Nieman et al. 1993; Schmetz et al. 1993).

As these two methods have been intensively used for operational applications, they have been regularly tested and studied for the two last decades. Indeed, cloud-top heights estimated from passive sensors have often been compared against lidar or radar measurements and have recently taken advantage of the synergy of the A-Train instruments. Weisz et al. (2007) compared the cloud-top heights estimated by the Atmospheric Infrared Sounder (AIRS), the Moderate Resolution Imaging Spectrometer (MODIS), *CloudSat*, and the Cloud-Aerosol Lidar with Orthogonal Polarization (CALIOP); Zhang and Menzel (2002) proposed an improvement in the CO_2-slicing method applied to thin cirrus, comparing the MODIS Airborne Simulator (MAS) and the Cloud Lidar System (CLS), which has been implemented operationally to set the altitude of the AMVs extracted from Geostationary Operational Environmental Satellite (GOES) instrumentation; Berthier et al. (2008) compared cloud statistics from the National Aeronautics and Space Administration's (NASA) Lidar in Space Technology Experiment (LITE), NASA's Geoscience Laser Altimeter System (GLAS), CALIOP, and MODIS; Menzel et al. (2008) compared MODIS cloud-top pressures with airborne lidar, CALIOP, and the High Resolution Infrared Radiation Sounder (HIRS); and Sèze et al. (2008) compared several AMV HA methods used at EUMETSAT, especially STC and CO_2-slicing methods, with collocated CALIOP data. These references are not exhaustive and represent a small part of the corresponding cloud-top pressure literature. However, it illustrates well that an accurate retrieval of cloud-top pressure from passive sensors is still the subject of ongoing research.

There are both scientific and technical reasons that make the study and validation of cloud-top pressure retrieval from a passive sensor very difficult. The optical thicknesses of semitransparent clouds can be very small (e.g., 0.1 or 0.2) but their geometrical depths quite large (e.g., 2–3 km or more). In contrast to thick opaque clouds, for which a clear separation exists between the cloud top and the clear air above, a physical definition itself of the top of semitransparent clouds is very difficult, as it is directly linked to the characteristics of the instrument used to observe it. For example, due to the nature of infrared measurements, the ability to retrieve altitudes of optically thin cirrus clouds is more limited than using lidar instrument. Comparing lidar instruments themselves, optically thin cirrus clouds are better identified from LITE profiles than with other lidars due to their higher signal to noise ratios (Berthier et al. 2008). Despite their general good agreement, AIRS is better suited to retrieve thin cirrus than MODIS (Weisz et al. 2007). Therefore, the results of these comparisons should always be analyzed with care as the characteristics of the instruments are different. Different observation spatial resolutions can also impact the cloud-top pressure retrieval in cases of broken clouds of small horizontal extent.

To alleviate the question of the real location of the cloud top and to complement the statistics and studies based on satellite observations, this study uses simulated data. The use of simulated radiances also provides the big advantage by comparing the pressure estimated by the HA method to the initial pressure set to the cloud in the model, which is exactly known, and to study the relative impact of several atmospheric or microphysical parameters. The radiative transfer code FASDOM (Dubuisson et al. 2005) has been used to simulate MSG radiances for various types of clouds at different levels in the troposphere, using several atmospheric profiles.

This paper first describes the two cloud-top height techniques and the simulated dataset used to generate Spinning Enhanced Visible and Infrared Imager (SEVIRI) radiances with FASDOM. The sensitivity of the HA results to several atmospheric parameters is then presented for gray clouds, for which the extinction coefficient has no spectral variation. These results give information regarding the performance of these methods, applying them in perfectly well-known atmospheric conditions. In a second step, more realistic ice clouds with spectrally varying optical properties are used to test the

methods, showing different results than for gray clouds. Some of the trends already noted using satellite observations are confirmed by using the simulated radiances, and may be then explained more precisely by their sensitivity to cloud microphysics. The next section discusses the performance of the HA methods when realistic perturbations are introduced into the atmospheric temperature and humidity profiles, and also on the clear-sky radiance values.

The occurrence of multilayer situations is very high when tracking AMVs with geostationary satellites, and these cases are difficult to treat. Comparing AMV HA methods with collocated CALIOP measurements, Sèze et al. (2008) showed that for nearly 35% of the low-level AMVs the lidar detected another cloudy layer at middle or high levels located at the same place. The FASDOM radiative transfer model can consider two different cloudy layers, which allows us to estimate the impacts on the retrieved cloud-top pressure of thin cirrus above an opaque cloud. The last part of this paper discusses this impact as a function of the upper cirrus optical thickness.

2. Cloud-top height techniques

a. Semitransparency correction method (STC)

The STC method exploits the fact that water vapor radiances vary linearly against IR window radiances as a function of the cloud amount to extrapolate the cloud height (Szejwach 1982; Nieman et al. 1993; Schmetz et al. 1993). This means that the relation between the radiance measured with the WV6.2 and IR10.8 channels is approximately linear for a semitransparent cloud. Figure 1 illustrates this relationship for a 24 × 24 target area used to extract AMVs from the *Meteosat-8* satellite. The left side of Fig. 1 presents the infrared 10.8-μm image radiance of the corresponding target area, which contains a large semitransparent cloud (in black in the image). This scene has been taken at 0230 UTC 1 December 2002, at 10.5°N and 19.66°E. Technically, the pixels inside the target area are sorted into several clusters considering microphysical and/or radiative properties and the calculation can be done for all the clusters. Borde and Oyama (2008) show that the pixel selection process is a key issue in the AMV extraction scheme, and the criteria used for the clustering must be chosen carefully. The right side of Fig. 1 shows an example for which the clustering has been performed considering various percentages of the coldest cloudy pixels present in the target area. The black solid curve represents the WV7.3 and IR10.8 radiances as calculated by a radiative transfer model for an opaque cloud at various pressure levels in the atmosphere. Temperature and humidity profiles extracted from a forecast model are used in the radiative transfer code. The cloud-top pressure of the semitransparent cloud is estimated from the intersection of the straight line defining the relation between the clear sky [asterisk (*)] and cluster representative radiances with the calculated curve for opaque clouds. If the intersection point is found above the tropopause level, the cloud top is assigned to the pressure at the tropopause. The method is regarded as failed if no (nominal) intersection point can be found. The two following combinations of channels are studied below: WV6.2 and IR10.8 and WV7.3 and IR10.8.

b. CO_2-slicing method

In the CO_2-slicing technique (Smith and Platt 1978; Menzel et al. 1983; Eyre and Menzel 1989; Nieman et al. 1993), a cloud height is assigned with the ratio of the deviation in the observed radiances from the corresponding clear-air radiances for the infrared window IRν (IR10.8 or/and IR12.0) and the CO_2 (IR13.4 μm) channel. The general equation for the CO_2-slicing technique is

$$\frac{R_{\mathrm{cf}}(\mathrm{CO_2}) - R_{\mathrm{cd}}(\mathrm{CO_2})}{R_{\mathrm{cf}}(\mathrm{IR}\nu) - R_{\mathrm{cd}}(\mathrm{IR}\nu)} = \frac{\varepsilon(\mathrm{CO_2})}{\varepsilon(\mathrm{IR}\nu)} \frac{[R_{\mathrm{suf}}(\mathrm{CO_2}) - R_{\mathrm{bcd}}(\mathrm{CO_2}, P_c)]}{[R_{\mathrm{suf}}(\mathrm{IR}\nu) - R_{\mathrm{bcd}}(\mathrm{IR}\nu, P_c)]}, \quad (1)$$

where R_{cf} and R_{cd} are, respectively, the cloud-free and cloudy radiances. In addition, R_{suf} and $R_{\mathrm{bcd}}(P_c)$ are, respectively, the surface radiance and the Planck blackbody radiance for a black cloud at the level P_c in the atmosphere. These radiances are calculated with a radiative transfer model, based on NWP forecast temperature and humidity profiles. Here, $\varepsilon(\mathrm{CO_2})$ and $\varepsilon(\mathrm{IR}\nu)$ are the cloud emissivities in the two bands. These emissivities are generally considered to be identical in the two bands and are then ignored in the calculations. However, Zhang and Menzel (2002) showed that the impact of this cloud emissivities assumption on the retrieved cloud-top pressure is large, especially for thin cirrus clouds. The left side of Eq. (1) corresponds to SEVIRI observations, and the right side to radiative transfer calculations. Cloud-top pressure within the field of view can be specified as the ratio of cloudy and clear-sky radiance differences. The observed ratio of the differences is compared to a series of radiative transfer calculations at various cloud pressures P_c, and the cloud top is assigned the pressure that best satisfies the observations. The following combinations of channels are studied in the following: CO_2 10.8

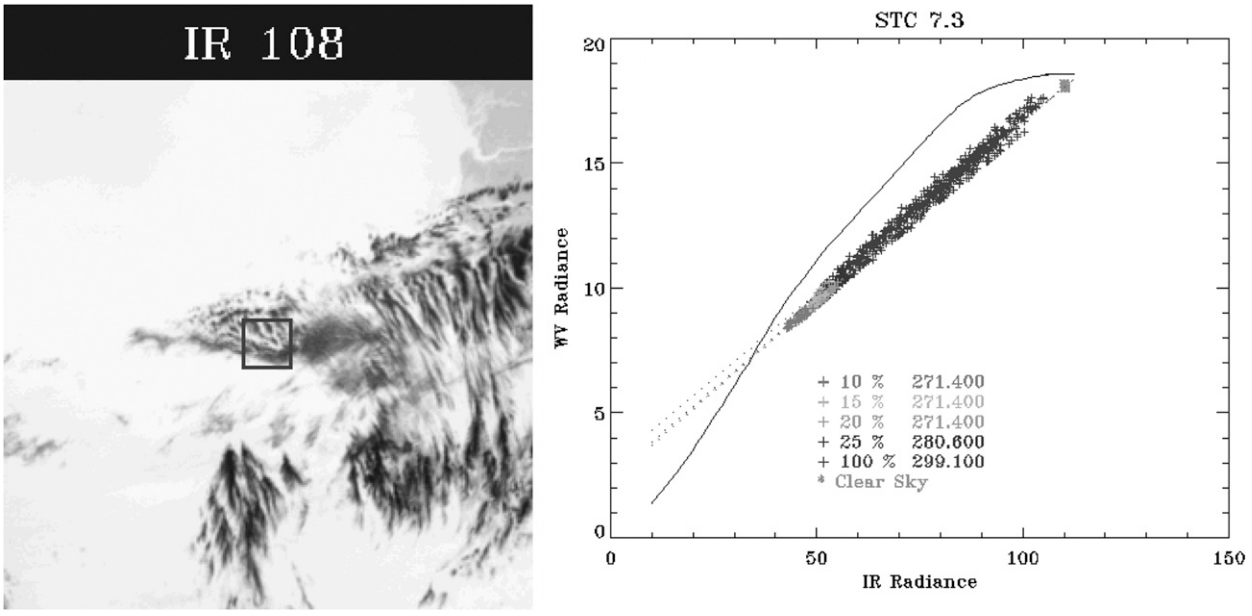

FIG. 1. Examples of the STC method that uses channels IR10.8 and WV7.3 applied to the 24 × 24 pixels target area illustrated in the Meteosat image on the left (taken at 0230 UTC 1 Dec 2002, at 10.5°N, 19.66°E). The different pressures have been retrieved using 10%, 15%, 20%, 25%, and 100% of the coldest cloudy pixels (in black on the image) present within the target area. The black solid curve represents the WV7.3 and IR10.8 radiances as calculated by a radiative transfer model for an opaque cloud at various pressure levels in the atmosphere.

that uses IR13.4 and IR10.8, and CO_2 12.0 that uses IR13.4 and IR12.0.

3. Simulated dataset description

One-dimension radiative transfer simulations have been performed for vertically inhomogeneous atmospheres using the fast but accurate radiative transfer code FASDOM (Dubuisson et al. 2005). It has been adapted to simulate MSG radiances or brightness temperatures in the following channels: WV6.2, WV7.3, IR10.8, IR12.0, and IR13.4 μm. The code is based on the discrete ordinates method (DOM) to solve the radiative transfer equation (Stamnes et al. 1988). Gaseous absorption is treated with the correlated *k*-distribution method, a method that accurately accounts for multiple scattering effects. Coefficients for the *k* distribution have been calculated (and tabulated) from a line-by-line code (Dubuisson et al. 2005), using the High-Resolution Transmission Molecular Absorption (HITRAN) spectroscopic database (2004) and the Clough–Kneizys–Davies (CKD) 2.4 water vapor continuum. The impacts of H_2O, CO_2, O_3, CH_4, and N_2O are considered in the calculations. Coefficients account for the spectral response of the MSG channels. The FASDOM code has been compared with the LBLDOM reference code. The differences between the brightness temperatures are generally less than 0.1 K.

The radiative transfer equation is solved in the plane-parallel approximation, assuming an atmosphere stratified into 39 layers. Eight atmospheric profiles have been selected from the Thermodynamic Initial Guess Retrieval (TIGR) database (Chevallier et al. 1998; Chedin et al. 1985) in order to be representative of low or medium latitudes. Clouds are defined by their optical properties: optical thickness δ, single scattering albedo ϖ, and asymmetry factor *g*. Different types of homogeneous and totally overcast clouds (cloud fraction equal to 1) have been selected with spectral properties for a liquid cloud using Mie theory (Stephens 1979) or assuming nonspherical crystals (Baum et al. 2005). The spectral dependence of the extinction coefficient is linked to the microphysical properties of the cloud. Figure 2 illustrates this variation for cloud cases used in the FASDOM simulations: a liquid cloud having 6-μm droplets and four ice clouds having 10-, 20-, 40-, and 80-μm ice crystals, respectively. Extinction coefficients are normalized to 1 in the CO_2 13.4-μm channel. Spectrally neutral Lambertian dark surfaces have been considered (surface emissivity = 1). Test cases are summarized in Table 1.

In the statistics presented below, ice clouds have been considered only for temperature $T < 253$ K, and a maximum optical thickness equal to 16. Liquid clouds have been considered only for temperature $T > 253$ K.

Considering cloud fractions smaller than 1 should place the cloud-top height a bit lower in the troposphere than

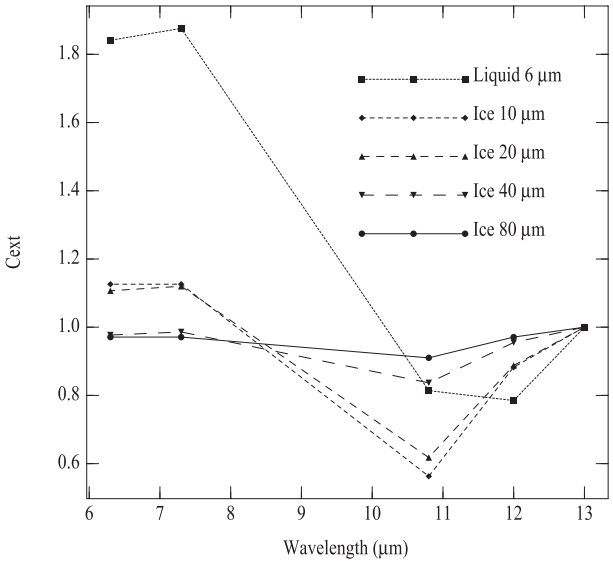

FIG. 2. Spectral variation of the extinction coefficient for the simulated liquid (Stephens 1979) and ice clouds (Baum et al. 2005) used in the simulation dataset described in Table 1.

using a cloud fraction equal to 1, as the radiance composed by both the surface and the cloud is larger than the radiance of the cloud itself. However, it should be noted that 1) it is currently not possible to get accurate information of the cloud fraction of Meteosat cloudy pixels that could be used further in AMV height assignment calculations and 2) the selection of the pixels used for the AMV height-assignment process generally favors the coldest pixels in the 24×24 target box, which mainly correspond to overcast situations. The impacts of the cloud fraction appear then to be very limited within the framework of this study and justify the use of a cloud fraction equal to 1.

4. Performances of the methods in idealized situations

a. Gray clouds

To test the intrinsic HA methods' accuracy, these methods have been applied to ideal gray clouds for which the extinction coefficient does not vary as a function of the wavelength. In the following the graphs mainly present the difference of the pressure $\Delta P = P(\text{retrieved}) - P(\text{simulation})$ as a function of various parameters. This difference gives direct information on the technical capabilities of the methods to retrieve the correct cloud-top pressure defined in the simulation model. Figure 3 shows the results of this pressure difference plotted as a function of cloud optical thickness δ at 13 μm for several cases of a perfect gray cloud located at various levels in the troposphere. The left column in Fig. 3 illustrates the sensitivity of the STC method that use channels WV6.2 μm and IR10.8 μm for cloud depths equal to 2 km (top) and 1 km (bottom). Similarly, results are plotted on the right side in Fig. 3 for the CO_2-slicing method using channels IR13.4 μm and IR12.0 μm. The results of the other STC and CO_2-slicing configurations using channels at 7.3 μm instead of WV6.2 μm and IR10.8 μm instead of IR12.0 μm are very similar to the results presented in Fig. 3 and are therefore not shown. All the methods retrieved the pressure to within a few hectopascals for thick opaque clouds; the accuracy decreases up to nearly 45 hPa when the clouds are very thin, with an optical thickness of $\delta < 0.1$. The pressure difference is larger when the cloud top is lower in the troposphere. Indeed, as the cloud-top temperature becomes warmer, the contrast between the cloud and the surface becomes smaller, which makes the retrieval less accurate. However, the pressure difference ΔP is also large when the cloud top is high in the troposphere and close to the tropopause (solid line at 131 hPa in Fig. 3). All the methods overestimate the cloud-top pressure regardless of the configuration used, setting the cloud-top height slightly too low in the troposphere. The density of the cloud impacts the results as well; the pressure difference being smaller for denser clouds for which the separation of the cloud and the clear air above the cloud is better defined. Here, ΔP is twice as large for clouds with vertical extents of 2 km (Fig. 3, top) instead of 1 km (Fig. 3, bottom) for clouds having the same optical thickness. These results constitute a good sanity check of the methods' accuracy, applying them in ideal conditions.

TABLE 1. Description of the main inputs to the simulation dataset.

Input	Case
Atmospheric profiles	Midlatitude (4), tropical (4)
Clouds	Gray, liquid (6 μm), four crystal (10, 20, 40, and 80 μm)
Cloud optical thickness	0.2, 0.5, 1, 2, 4, 8, 16, 32, and 50 at 13 μm
Cloud-top pressure	11 cloud-top heights, from 525 to 106 hPa
View angle	$\theta = 0°$, 45°, and 60°

b. Clouds having spectral dependence of their extinction coefficient

A gray cloud is an ideal case study, and the spectral variation of natural clouds is linked to its microphysical properties. Figure 4 illustrates the pressure difference ΔP plotted as of function of various cloud microphysical properties: a gray cloud, a liquid cloud having 6-μm droplets that corresponds to altostratus characteristics, and four ice clouds having 10-, 20-, 40-, and 80-μm ice crystals, respectively. Results are presented only for the

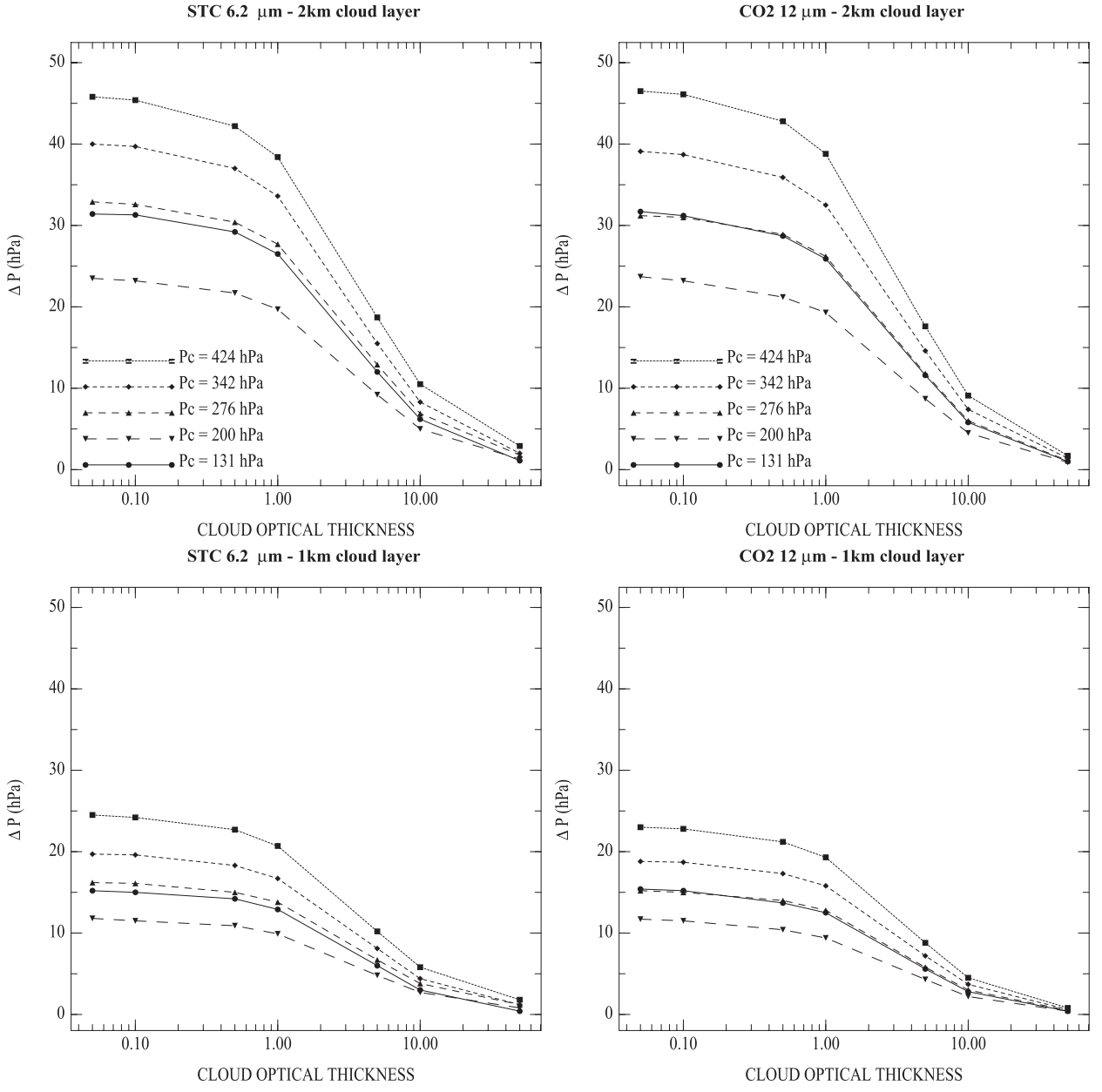

FIG. 3. Pressure difference, ΔP, defined as P(retrieved) $-$ P(simulation), plotted as a function of the gray clouds optical thickness at 13 μm, i.e., clouds having no spectral variation. The different lines correspond to various cloud-top pressures P_c.

STC6.2 and CO_2 IR12.0 configurations, for clouds having an optical thickness of $\delta = 2$, in a midlatitude atmosphere. The STC6.2 method generally slightly overestimates the retrieved cloud-top pressure of the ice clouds, setting the cloud top too low in the troposphere, whereas the CO_2-slicing method tends to underestimate the pressure, setting the cloud top too high. Absorption of ice particles is greater at the CO_2 wavelength IR13.4 μm than at the water vapor wavelength WV6.2 μm. As shown in Fig. 2, the STC technique is not as sensitive to ice and sees deeper into the cirrus before it responds. That trend was already obtained by Smith and Frey (1991) and Schreiner and Menzel (2002), who compared the two techniques using GOES instrumentation. In these studies the STC technique placed the top of the cirrus clouds lower in the troposphere by 80 hPa on average than did the CO_2-slicing method.

However, the STC6.2 method appears to be more accurate and more robust than the CO_2-slicing method when using this simulated dataset. This is the opposite of

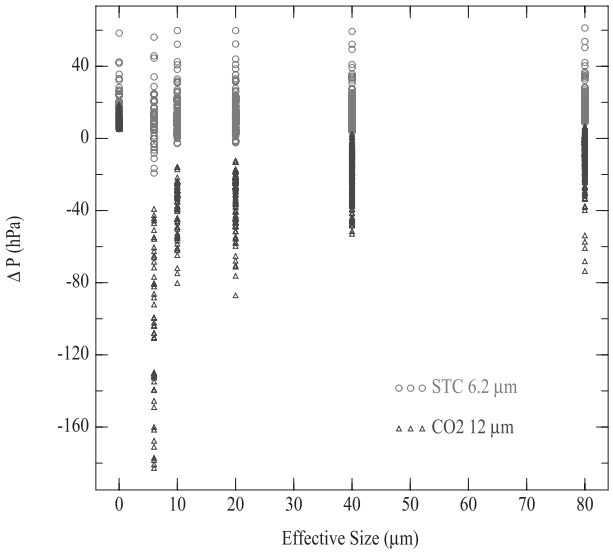

FIG. 4. Pressure difference, $\Delta P = P(\text{retrieved}) - P(\text{simulation})$, as a function of cloud microphysics: a liquid water cloud with 6-μm droplets and four ice clouds with effective sizes of 10-, 20-, 40-, and 80-μm ice crystals, respectively. A gray cloud case is plotted for comparison (value 0 on the x axis). Results correspond to simulations in a midlatitude summer atmosphere for a cloud having an optical thickness equal to 2 and a nadir view angle.

the result obtained operationally by Schreiner and Menzel (2002) using GOES instrumentation, which selected the CO_2-slicing method to set the AMV altitude in the AMV extraction algorithm. In our case, the CO_2-slicing method is more sensitive to the cloud phase and also to the ice particle size than is the STC technique. This difference may be explained by the large natural noise present in the real data, especially regarding the clear-sky radiance and humidity profile, which is not completely taken into account in the simulations. This question is discussed in more detail below in section 4.

More detailed statistics are presented in Table 2. The standard deviations (STDs), biases to real cloud-top pressure, and success rates (%) of the methods are presented for STC6.2 and CO_2 12.0, as a function of several pressure levels (Table 2, first column). Statistics are calculated for clouds having optical thicknesses varying from 1 to 50.

Table 2a presents results for gray clouds. Both STC6.2 and CO_2 12.0 retrieve the cloud-top pressure within a few hectopascals, and have small standard deviations. As noted in Fig. 3, they systematically overestimate the pressure, setting the cloud top slightly too low in the troposphere. The accuracy is worse for $P > 380$ hPa, especially for the STC6.2 method. The success rate, which illustrates the percentage of the cases for which the method succeeded in retrieving the cloud-top pressure, is very good except for the STC6.2 method at low levels ($P > 400$ hPa). It should be noted that retrieving a cloud-top pressure successfully does not mean that the result is good; it simply indicates that method did not fail technically in finding the result.

Table 2b shows the same statistics for more realistic ice clouds having 10-, 20-, 40-, and 80-μm ice crystals. The biases and standard deviations are smaller for the STC6.2 method than for the CO_2 12.0 method. The STC6.2 method tends to overestimate the cloud-top pressure by less than 6 hPa except for $P > 400$ hPa, for which the bias is larger. The success rate of the STC6.2 method is very good between 400 and 150 hPa. The CO_2 12.0 method tends to underestimate the cloud-top pressure by ~20 hPa on average, setting the cloud-top height a bit too high in the troposphere. Standard deviations are also large, between 30 and 45 hPa. The ΔP is smaller for high-level clouds above 160 hPa but the success rate of the CO_2 12.0 configuration is poor at these levels. Considering these idealized situations, the CO_2 12.0 method therefore appears to be generally less robust and less accurate than the STC6.2 method.

The spectral variation of the extinction coefficient is directly linked to the microphysical properties of the cloud as illustrated in Fig. 2. The extinction coefficient of large ice crystals has very little spectral variation, which bring these clouds close to the gray cloud's properties. At the opposite extreme, the extinction coefficient of ice clouds that contain small particles varies considerably as a function of the wavelength. Table 2c illustrates the same statistics as Table 2b, but while considering only small particles (10 and 20 μm). The results of the STC method are very similar to those of Table 2b, but the biases and standard deviations are larger for the CO_2-slicing method. At high levels both the biases and standard deviations are smaller, but the success rates are dramatically lower, down to 0 for the 106-hPa pressure level. The success rate of the STC method is also very poor at 106 hPa, which means that both methods frequently fail in retrieving a cloud-top pressure when the clouds are composed of small ice particles at 100 hPa. The results of the CO_2-slicing method are better for large ice particles (>20 μm), having a bias close to −15 hPa and a standard deviation around 20 hPa (not shown).

c. *Comparison of various configurations of the same method*

Considering the MSG channels, both the STC and CO_2-slicing methods can be applied following different combinations of channels. Figure 5 represents density plots of CO_2 10.8 pressures versus CO_2 12.0 pressures (top panel) and STC7.3 pressures versus STC6.2 pressures (bottom panel). The gray scale represents the dot density, given as the percentage of the total number of ice clouds simulations.

TABLE 2. Summary of performance (success rate; %) and accuracy (bias and std dev; hPa) of AMV HA methods using (a) single-layer gray clouds, (b) ice clouds (10-, 20-, 40-, and 80-μm ice particle sizes), and (c) ice clouds with small particles (<20 μm) from the simulated dataset described in Table 1.

	STC method			CO_2 method		
Cloud pressure level (hPa)	Std dev (hPa)	Bias (hPa)	Success rate (%)	Std dev (hPa)	Bias (hPa)	Success rate (%)
(a) Single-layer gray clouds						
471	24	16	68	11	8	100
423	16	12	95	9	7	100
380	10	8	100	8	6	100
342	8	6	100	7	5	100
307	7	6	100	7	5	100
276	7	5	100	6	4	100
247	7	5	100	6	4	100
222	6	4	100	5	4	100
200	5	4	100	4	3	100
162	8	6	100	8	6	100
131	6	5	100	6	4	100
106	5	4	100	5	4	100
(b) Ice clouds (10-, 20-, 40-, and 80-μm ice particle sizes)						
471	21	14	65	49	−26	99
423	20	12	94	47	−24	98
380	17	6	99	48	−24	98
342	9	6	100	37	−20	99
307	14	4	100	38	−22	98
276	7	2	100	36	−23	98
247	9	1	100	32	−19	96
222	7	0	100	27	−16	94
200	12	−1	99	26	−16	91
162	10	3	98	15	−9	86
131	23	2	96	9	−5	70
106	6	4	56	1	1	8
(c) Ice clouds with small particles (<20 μm)						
471	20	10	66	72	−45	98
423	19	7	94	69	−41	97
380	22	2	99	68	−40	96
342	7	2	100	52	−35	98
307	24	2	100	51	−37	96
276	7	−3	100	48	−35	95
247	8	−4	100	41	−28	92
222	10	−4	100	36	−25	89
200	16	−8	99	33	−24	85
162	11	−1	97	18	−13	77
131	25	1	91	10	−8	55
106	3	2	22	—	—	0

The cloud-top pressures retrieved by the two different configurations of the STC method are in general in good agreement. Above 400 hPa there is no bias between the STC6.2 and STC7.3 retrieved pressures. This can be explained by the quite neutral spectral variation of the extinction coefficient in these two water vapor channels for the clouds considered in the simulations (see Fig. 2). However some differences occur when the retrieval is more difficult for very thin clouds and/or clouds located at the lower levels; below 300 hPa. The pressure retrieved using the WV6.2 channel is then smaller than that retrieved using the WV7.3 channel, due to the impacts of water vapor located above the cloud. The WV7.3 channel is less sensitive than the WV6.2 channel to the humidity located at very high levels because its weighting function peaks lower in the troposphere (close to 550 hPa). Therefore, the WV6.2 radiance of very thin clouds located below the peak of the WV6.2 channel at 250 hPa is more significantly impacted by the water vapor located above the cloud, than the is radiance of the WV7.3 channel.

Pressures estimated by CO_2 12.0 are systematically larger than the pressures obtained from the configuration that uses the IR10.8 μm channel. The bias between

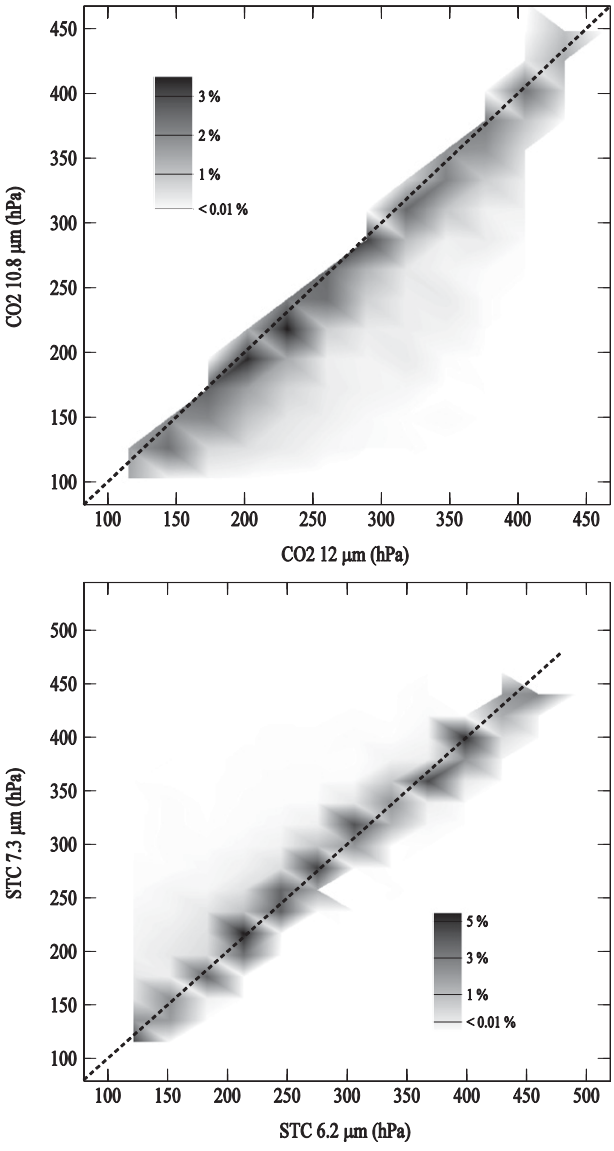

FIG. 5. Density plots of (top) CO_2 10.8 pressure vs CO_2 12 pressure and (bottom) STC7.3 pressure vs STC6.2 pressure. The gray scale represents the dot density, given in percent of the total number of ice clouds simulations.

the two CO_2-slicing configurations is nearly 20 hPa using the simulated radiance dataset. Borde and Arriaga (2004) showed this when comparing the results of AMV height assignment techniques used with *Meteosat-8* data. This difference is mainly due to the assumption considered in the CO_2-slicing Eq. (1), which assumes the emissivities in the IR and CO_2 channels to be equal. Also, the extinction coefficient of small ice particles is smaller at IR10.8 μm than at IR12.0 μm, which makes the cirrus clouds appear slightly "thinner" at 10.8 μm than at IR12.0 μm.

Zhang and Menzel (2002) proposed to improve the retrieval of the CO_2-slicing cloud-top pressure and the effective cloud amount by applying emissivity ratio adjustments. Within that framework they considered the CLS (Spinhirne and Hart 1990) cloud data to be the true reference value. Their new CO_2-slicing algorithm has been tested using the MODIS instrument and showed better agreement with lidar data for thin cirrus clouds. For a cloud emissivity ratio increase of 10% (longer wavelengths divided by shorter wavelengths, then 13.2/11.0, 13.7/13.2, and 14.2/13.7 μm using MAS CO_2 pairs), the cloud-top heights of thin clouds increased by 35 hPa. The effect of the new CO_2-slicing method on *GOES-8* Sounder data was studied, and the cloud-top height increase was ~10 hPa and the RMS difference was approximately 30 hPa for thin clouds (Zhang and Menzel 2002). Applying such an emissivity ratio adjustment, the new CO_2-slicing algorithm placed the clouds lower in the troposphere, which is in good agreement with the results of the CO_2-slicing method presented above using the simulated data.

5. Impacts of errors in the geophysical data

a. Error coming from atmospheric profiles

Monitoring statistics in forecast centers are calculated by comparing observations with 6-h model forecasts valid at the observation times. Both the observations and the model forecast contribute to the differences; neither can be assumed to be true. Such observation − background statistics show that the global RMS difference between radiosondes and a global NWP model is ~1 K for the temperature profile (lower in midtroposphere, but ~2 K near the surface) and ~13% for the relative humidity at low levels, rising to ~17% at ~800 hPa and peaking at more than 20% in the upper troposphere before falling rapidly above the tropopause (C. Parrett and R. Rawlins 2009, personal communication).

As NWP temperature and humidity profiles are used by the HA methods, sensitivity tests have been performed to estimate the impacts of these technical uncertainties on their performance. Perturbations have been added to the temperature (+0.5 K) and humidity profiles (+10%) from NWP, using perturbations that are constant in the vertical throughout the profile. While perturbations that are constant in the vertical do not necessarily represent typical individual errors in short-term forecasts, they nevertheless provide some estimate of the sensitivity of the height assignment to the errors in the atmospheric background profiles. Note, however, that errors in short-term forecasts typically have a more complicated structure in the vertical, and our choice of perturbation is likely to lead to an exaggerated estimate of the general short-term forecast error on the HA. Results are presented in Tables 3a and 3b, respectively, considering only gray clouds, in order to eliminate the uncertainties coming

TABLE 3. Average of errors ΔP_{pert} of the perturbed pressure minus unperturbed pressure (hPa) for the HA methods when varying the temperature profile by 0.5 K and varying the humidity profile by +10%.

Cloud pressure level (hPa)	δ	ΔP_{pert} (hPa) STC6.2	ΔP_{pert} (hPa) STC7.3	ΔP_{pert} (hPa) $CO_2$10.8	ΔP_{pert} (hPa) $CO_2$12.0
Varying the temperature profile by 0.5 K					
424	0.25	−66	−34	−22	−26
	0.50	−36	−16	−10	−12
	1.00	−16	−6	−4	−5
	2.00	−4	−2	−1	−1
342	0.25	−44	−28	−12	−16
	0.50	−19	−12	−5	−7
	1.00	−7	−4	−2	−3
	2.00	−2	−1	−1	−1
276	0.25	−49	−38	−12	−17
	0.50	−23	−16	−5	−7
	1.00	−8	−6	−2	−3
	2.00	−2	−2	−1	−1
223	0.25	−51	−32	−7	−11
	0.50	−19	−16	−3	−5
	1.00	−7	−6	−1	−2
	2.00	−2	−2	0	−1
162	0.25	−29	−32	−5	−10
	0.50	−24	−15	−2	−6
	1.00	−10	−10	−1	−2
	2.00	−3	−3	0	−1
106	0.25	—	—	−1	−2
	0.50	−10	−10	−1	−4
	1.00	−6	−6	0	−1
	2.00	−3	−3	0	0
Varying the humidity profile by +10%					
424	0.25	250	83	57	46
	0.50	116	34	25	20
	1.00	29	13	10	8
	2.00	5	3	3	2
342	0.25	68	57	37	27
	0.50	27	26	16	11
	1.00	10	10	6	4
	2.00	3	3	2	1
276	0.25	60	65	35	24
	0.50	29	33	16	11
	1.00	13	14	7	4
	2.00	3	4	2	1
223	0.25	71	77	34	19
	0.50	30	35	13	8
	1.00	11	14	5	3
	2.00	3	4	1	1
162	0.25	66	80	26	17
	0.50	31	42	13	8
	1.00	14	20	6	4
	2.00	5	7	2	1
106	0.25	71	103	28	19
	0.50	35	58	13	7
	1.00	15	29	6	3
	2.00	4	10	1	1

from the spectral cloud properties. Table 3 presents the average of errors, ΔP_{pert}, of the perturbed and unperturbed pressure differences for various cloud optical thicknesses (from 0.25 to 2) and various levels in the troposphere (from 424 to 106 hPa). The unperturbed pressures are not the true pressure set to the cloud in the simulations, but the pressures retrieved by the methods when the NWP profiles are not modified. Therefore the ''perturbed minus unperturbed'' differences give direct estimates of the errors coming from the perturbations of the NWP data profiles. Statistics have also been calculated for clouds having an optical thickness larger than 2 (not shown), and their magnitudes were close to zero for both Tables 3a and 3b. The CO_2-slicing configurations appear to be more robust than the STC configurations to a 0.5-K variation of the temperature profile. The largest impact occurs for the STC6.2 configuration. Large ΔP_{pert} corresponds generally to very thin clouds, having an optical thickness smaller than 0.5.

All the studied methods are impacted by a +10% variation of the humidity profile, especially the two STC configurations. The impact is large for thin clouds that have an optical thickness smaller than 0.5, for which the ΔP_{pert} are reaching several tens of hectopascals. The STC6.2 method is slightly more accurate at high levels above 250 hPa than the STC7.3 configuration, while the opposite holds true below 250 hPa. The CO_2-slicing configurations are more robust than the STC ones to this perturbation introduced in the humidity profile. It should be noted that all the differences are positive considering such a +10% positive perturbation, which tends to shift the cloud-top pressure too low in the troposphere. Results have the same order of size but opposite sign, considering a negative bias in the humidity profile and in the temperature profile (results not shown). The accuracy of the humidity profiles in the NWP models (C. Parrett and R. Rawlins 2009, personal communication) constitutes one of the main potential sources of errors when using HA methods operationally to set the AMV altitude.

b. Error coming from clear-sky radiance

When no clear-sky pixels are identified within the 24×24 target area used to extract AMVs from satellite images, the clear-sky representative radiance used in the HA methods is obtained from the forecast profile. This means that the end of the solid line curve is considered for the calculations instead of the clear-sky pixels [asterisk (*); upper-right symbol grouping] plotted in Fig. 1. Of course, such a process is also a source of error as the surface radiance calculated from the forecast fields can be slightly different than the ones retrieved from the satellite data. Moreover, even if clear-sky pixels are identified within the target box, they do not always correspond

exactly to the end of the solid curve in Fig. 1, where they are supposed to be. The differences may come from the uncertainties of the NWP temperature profiles and surface temperature values, from the uncertainties in clear-sky pixel identification using satellite observations, from radiative transfer errors (spectroscopy, layering, response function used), from the quality of the calibration, and also because the solid line in Fig. 1 is calculated at a fix grid point of the NWP model that does not correspond exactly to the geographical location of the detected AMV. Table 4 illustrates the impacts of a 10% reduction of the clear-sky radiance on the HA methods. Only gray clouds have been considered in this statistic in order to alleviate the potential impacts coming from the microphysics spectral properties. The average of the errors ΔP_{pert} of the perturbed and unperturbed pressure differences are presented for various cloud optical thicknesses, varying from 0.25 to 2, and several pressure levels, from 424 to 106 hPa. Calculations have also been performed for clouds having an optical thickness larger than 2 and all the biases were very close to zero.

The CO_2-slicing configurations are more sensitive to the variation of the clear-sky surface radiance than are the STC ones. Biases are very large for very thin clouds ($\delta < 1$), reaching 250 hPa and nearly 300 hPa for CO_2-slicing methods at the 162- and 106-hPa pressure levels, respectively. Although remaining very large, biases obtained using STC configurations tend to be smaller when the pressure levels are decreasing from 424 to 106 hPa. It is the opposite for CO_2-slicing configurations, which appear to be more significantly impacted by a variation in the clear-sky radiance when the cloud is at very high levels in the troposphere. Even for clouds that have an optical thickness equal to 1, the biases given by CO_2-slicing configurations are quite large at high levels, close to 40 hPa at the 162-hPa pressure level, and 50 hPa at the 106-hPa pressure level. Both the STC and CO_2-slicing methods give positive ΔP_{pert} when applying this 10% reduction on the clear-sky radiance, setting the retrieved cloud-top pressure too low in the troposphere.

TABLE 4. Average of errors ΔP_{pert} of the perturbed pressure minus the unperturbed pressure (hPa) for the HA methods when varying the clear-sky surface radiance by 10%.

Cloud pressure level (hPa)	δ	ΔP_{pert} (hPa) STC6.2	ΔP_{pert} (hPa) STC7.3	ΔP_{pert} (hPa) $CO_2$10.8	ΔP_{pert} (hPa) $CO_2$12.0
424	0.25	97	97	—	—
	0.50	68	48	62	62
	1.00	34	16	27	27
	2.00	11	7	10	9
342	0.25	130	111	—	—
	0.50	56	26	65	64
	1.00	15	11	23	22
	2.00	7	5	9	8
276	0.25	151	73	157	157
	0.50	33	22	65	63
	1.00	15	11	26	25
	2.00	7	6	11	11
223	0.25	135	67	198	196
	0.50	40	28	78	76
	1.00	17	10	36	35
	2.00	7	5	11	11
162	0.25	122	61	246	241
	0.50	45	23	96	93
	1.00	22	14	39	38
	2.00	12	9	17	17
106	0.25	111	58	306	299
	0.50	45	30	114	112
	1.00	23	14	49	48
	2.00	12	9	19	19

6. Multilayer situations

Using LITE observations, Stubenrauch et al. (2005) found 55% of clouds are multilayer over land and 38% over ocean. In addition, 76% of the identified high clouds appeared with lower clouds underneath. Nazaryan et al. (2008) estimated the cirrus occurrence frequency for multilayer clouds using CALIOP observations. Multilayer cloud occurrences have been found to be very frequent in tropical areas, with a maximum occurrence of multilayer cirrus clouds up to 94% near the tropics over the 100°E–180° band. Hence, satellite systems with retrieval methods that assume single-layer clouds do not provide the correct cloud-top height information in multilayer situations. According to Chang and Li (2005), use of such cloud-top data would underestimate low clouds by ~30% if there were cirrus overlapping and the optical depths of the overlapped cirrus clouds would be overestimated by a factor of 7 because of the optically thicker water clouds underneath.

Indeed, using 24×24 pixel target boxes to track AMVs with geostationary satellites, the probability of having multilayer situations within the box is very high. Comparing AMV HA methods against collocated CALIOP measurements, Sèze et al. (2008) showed that for nearly 35% of the low-level AMVs the lidar detected another cloud layer at a middle or high level located at the same place. These cases are very difficult to treat operationally, first because the motion detected by the AMV algorithm can sometimes be a combination of the respective movements of the two layers, and second because the highest layer is often a semitransparent cloud for which the detection of the cloud-top height is very difficult.

The FASDOM code can perform the radiative transfer calculation considering two different cloudy layers, which allows us to estimate the impacts of thin cirrus located above an opaque cloud on the retrieved cloud top.

Figure 6 shows the differences ΔP between the pressures retrieved by the STC or CO_2-slicing methods and the cloud-top height set to the lowest cloudy layer in the FASDOM model. These differences are presented as a function of the optical thickness of the upper cirrus layer varying from 0.001 to 50, for two cases of cloudy layers separated by 2 km (plus signs) and 7 km (filled circles), respectively. Therefore, a value $\Delta P = 0$ means that the cloud-top pressure of the lowest layer is perfectly retrieved, and the values $\Delta P = -250$ hPa and $\Delta P = -70$ hPa correspond to perfect cloud-top retrievals of the two different highest cirrus layers considered, respectively.

Not surprisingly, when the upper cirrus cloud is very thin ($\delta < 0.1$), the cloud top of the lowest opaque layer is correctly retrieved by the two methods. However, a cirrus cloud having an optical thickness equal to 0.1 already impacts the retrieval, setting the cloud top of the lowest layer 30 hPa too high in the troposphere when the two layers are separated by 7 km. Although such cirrus is probably too thin to realistically be used by the tracking algorithm that employs the IR10.8 channel, it impacts the pressure retrieval of the actually tracked cloudy layer. When the cirrus optical thickness varies from 0.05 to 10, the HA methods place the cloud-top pressure somewhere between the two layers, depending on the cirrus optical thickness, on the geometrical distance between the two clouds, and on other atmospheric parameters. Results are then scattered over several tens of hectopascals for cirrus cloud having an optical thickness equal to 1, for example. The top of the cirrus cloud is accurately retrieved only when the cirrus optical thickness is larger than 10. However, these retrievals remain inaccurate for the CO_2-slicing method, whatever the distance between the two cloudy layers. The HA methods do not work properly in multilayer situations, and they are not able to provide usable information on cloud-top height for any upper cirrus optical thicknesses varying from 0.05 and 10. Most natural cirrus situations are included between these two values.

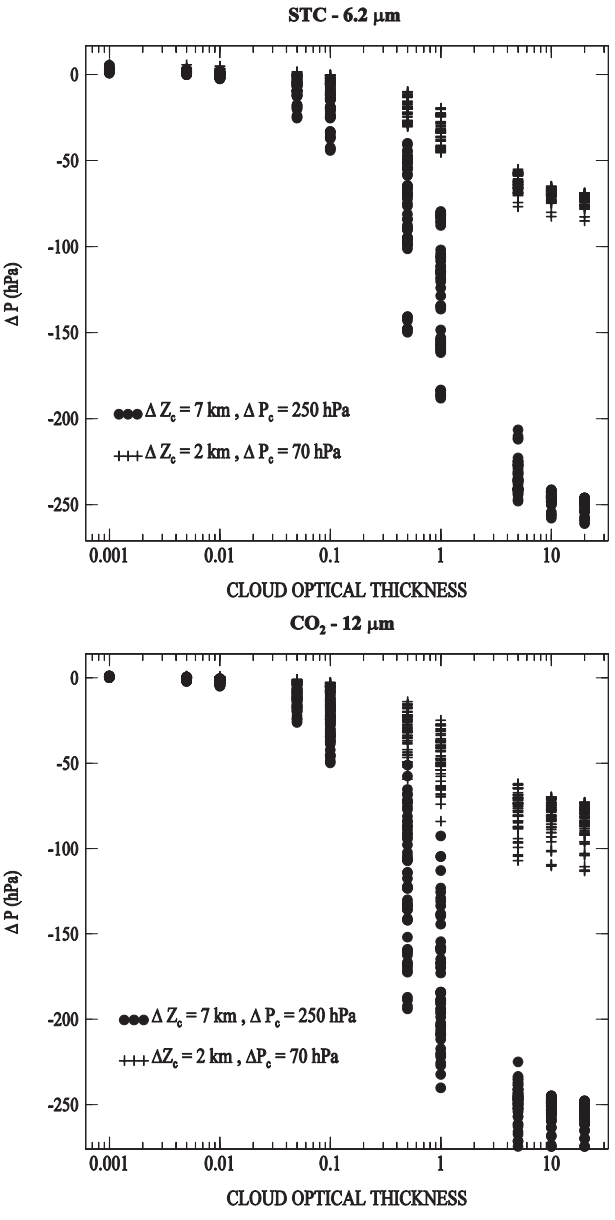

FIG. 6. Multilayer situations for which thin cirrus clouds are above a lower cloudy layer located 2 km (plus signs) and 7 km (filled circles) below. Pressure difference ΔP defined as the difference between the retrieved pressure and the pressure set to the top of the lowest layer in the simulation, is presented as a function of the upper cirrus optical thickness.

7. Discussion

This paper presents results on the sensitivity of CO_2-slicing and STC methods to several atmospheric parameters using simulated *Meteosat-8* radiances calculated by the FASDOM radiative transfer code. This study is realized within the framework of operational extraction of AMVs at EUMETSAT, in which these methods are intensively used to set the altitude of the wind vectors. The use of simulated radiances alleviates the problem of the absolute reference and illustrates the sensitivity of the methods to several atmospheric parameters. Both the STC and CO_2-slicing methods retrieve the correct pressure of a thick gray cloud within a few hectopascals. The CO_2-slicing method generally underestimates the retrieved pressure for more realistic clouds, which tends to set the cloud slightly too high in the atmosphere. The methods are sensitive to all of the tested atmospheric parameters, which makes accurate operational use very difficult. Cloud microphysics is an especially important

parameter that significantly impacts the performance of the CO_2-slicing method. Using this simulated dataset, the STC configuration, which uses the channel at WV6.2, finally appeared to be the most robust and most accurate method. However, both the STC and CO_2-slicing methods perform poorly in cases of thin clouds.

Perturbations in the atmospheric temperature and humidity profiles can greatly impact the results of the HA methods. The STC configurations appear less robust than the CO_2-slicing configurations to such perturbations. Pressure differences between the perturbed and unperturbed pressures can reach several tens of hectopascals for thin cirrus clouds that have an optical thickness smaller than 2. The considered +10% positive perturbation introduced in the humidity profile tends to set the cloud top too low in the troposphere, whereas a 0.5 K positive perturbation in the temperature profile sets the cloud top too high. Changing the sign of the perturbations in the profiles also changes the sign of the pressure differences. Reducing by 10% the values of the clear-sky radiance used in the STC and CO_2-slicing methods impacts the pressure retrieval by several tens of hectopascals for thin clouds. The CO_2-slicing method appears to be less robust to such variations, especially for thin clouds at high levels in the troposphere. The cloud-top pressure is biased toward the lower levels, setting the cloud top too low.

In summary, the accuracy and robustness of the STC method appears better in idealized situations, but this method is also more impacted than the CO_2 method by geophysical errors in the water vapor and temperature profiles. This can make the use of the STC method more difficult and unsecured for operational purposes.

An adequate correction of all the effects described above is not trivial because accurate retrieval of cloud microphysics is also very difficult using passive sensors. However the optimal cloud analysis scheme (Watts et al. 1998), currently in development at EUMETSAT, aims to accurately estimate the cloud optical depth, phase, cloud particle size, and pressure on a pixel-by-pixel basis. Such microphysical information should then be used operationally in the future to improve the performance of the AMV HA methods or to estimate the quality of the retrieval.

Sensitivity tests have been performed considering multilayer cloud situations, which show that neither the STC nor CO_2-slicing methods work properly in such cases, placing the cloud-top height somewhere between the two cloudy layers. The bias in cloud-top heights depends both on the upper cirrus optical thickness and on the vertical distance between the two layers. The retrieved pressure levels are not correct for all upper cirrus layers that have an optical thickness between 0.1 and 10, which unfortunately includes the largest proportion of natural cirrus clouds. There is currently no method that gives good cloud-top height estimations in multilayer situations using Meteosat data. Therefore, a method that can at least identify and flag these multilayer situations should be very helpful for operational purposes because then those data could be flagged as doubtful.

REFERENCES

Baum, B. A., P. Yang, A. J. Heymsfield, S. Platnick, M. D. King, Y.-X. Hu, and S. T. Bedka, 2005: Bulk scattering models for the remote sensing of ice clouds. Part II: Narrowband models. *J. Appl. Meteor.,* **44,** 1896–1911.

Berthier, S., P. Chazette, J. Pelon, and B. A. Baum, 2008: Comparison of cloud statistics from spaceborne lidar systems. *Atmos. Chem. Phys. Discuss.,* **8,** 6965–6977.

Borde, R., and A. Arriaga, 2004: Atmospheric motion vectors height assignment techniques with Meteosat-8. *Proc. Seventh Int. Winds Workshop,* Helsinki, Finland, EUMETSAT, 139–146.

——, and R. Oyama, 2008: A direct link between feature tracking and height assignment of operational atmospheric motion vectors. *Proc. Ninth Int. Winds Workshop,* Annapolis, MD, EUMETSAT. [Available online at http://www.eumetsat.int/Home/Main/AboutEUMETSAT/Publications/ConferenceandWorkshopProceedings/2008/groups/cps/documents/document/pdf_conf_p51_s3_13_borde_v.pdf.]

Chang, F.-L., and Z. Li, 2005: A near-global climatology of single-layer and overlapped clouds and their optical properties retrieved from *Terra*/MODIS data using a new algorithm. *J. Climate,* **18,** 4752–4771.

Chedin, A., N. A. Scott, C. Wahiche, and P. Moulinier, 1985: The improved initialization inversion method: A high resolution physical method for temperature retrievals from satellites of the TIROS-N series. *J. Climate Appl. Meteor.,* **24,** 128–143.

Chevallier, F., F. Cheruy, N. A. Scott, and A. Chedin, 1998: A neural network approach for a fast and accurate computation of longwave radiation. *J. Appl. Meteor.,* **37,** 1385–1397.

Dubuisson, P., V. Giraud, O. Chomette, H. Chepfer, and J. Pelon, 2005: Fast radiative transfer modeling for infrared imaging radiometry. *J. Quant. Spectrosc. Radiat. Transf.,* **95,** 201–220.

Eyre, J. R., and W. P. Menzel, 1989: Retrieval of cloud parameters from satellite sounder data: A simulation study. *J. Appl. Meteor.,* **28,** 267–275.

Forsythe, M., and M. Doutriaux-Boucher, 2005: Second analysis of the data displayed on the NWP SAF AMV monitoring website. NWP SAF Technical Rep. 20, Met Office, Reading, United Kingdom, 46 pp. [Available online at http://www.metoffice.gov.uk/research/interproj/nwpsaf/satwind_report/nwpsaf_mo_tr_020.pdf.]

Holmlund, K., 2000: The Atmospheric Motion Vector retrieval scheme for Meteosat Second Generation. *Proc. Fifth Int. Winds Workshop,* Lorne, Australia, EUMETSAT, EUM-P28, 201–208.

Le Marshall, J., N. Pescod, A. Khaw, and G. Allan, 1993: The real-time generation and application of cloud-drift winds in the Australian region. *Aust. Meteor. Mag.,* **42,** 89–103.

Menzel, W. P., W. L. Smith, and T. Stewart, 1983: Improved cloud motion wind vector and altitude assignment using VAS. *J. Climate Appl. Meteor.,* **22,** 377–384.

——, and Coauthors, 2008: MODIS global cloud-top pressure and amount estimation: Algorithm description and results. *J. Appl. Meteor. Climatol.,* **47,** 1175–1198.

Nazaryan, H., M. P. McCormick, and W. P. Menzel, 2008: Global characterization of cirrus clouds using CALIPSO data. *J. Geophys. Res.,* **113,** D16211, doi:10.1029/2007JD009481.

Nieman, N. J., J. Schmetz, and W. P. Menzel, 1993: A comparison of several techniques to assign heights to cloud tracers. *J. Appl. Meteor.,* **32,** 1559–1568.

Schmetz, J., K. Holmlund, J. Hoffman, B. Strauss, B. Mason, V. Gärtner, A. Koch, and L. Van de Berg, 1993: Operational cloud motion winds from Meteosat infrared images. *J. Appl. Meteor.,* **32,** 1206–1225.

——, P. Pili, S. Tjemkes, D. Just, J. Kerkmann, S. Rota, and A. Ratier, 2002: An introduction to Meteosat Second Generation (MSG). *Bull. Amer. Meteor. Soc.,* **83,** 977–992.

Schreiner, A. J., and P. Menzel, 2002: Comparison of cloud motion vector height assignment techniques using GOES-12 imager. *Proc. Sixth Int. Winds Workshop,* Madison WI, EUMETSAT, 301–305.

Sèze, G., S. Marchand, J. Pelon, and R. Borde, 2008: A comparison of AMV cloud top pressure derived from MSG with space-based lidar observations. *Proc. Ninth Int. Winds Workshop,* Annapolis, MD, EUMETSAT.

Smith, W. L., and C. M. R. Platt, 1978: Intercomparison of radiosonde, ground based laser, and satellite deduced cloud heights. *J. Appl. Meteor.,* **17,** 1797–1802.

——, and R. Frey, 1991: Altitude specification of cloud motion winds. *Proc. Workshop on Wind Extraction from Operational Meteorological Satellite Data,* Washington, DC, EUMETSAT, 189–198.

Spinhirne, J. D., and W. D. Hart, 1990: Cirrus structure and radiative parameters from airborne lidar and spectral radiometer observations. *Mon. Wea. Rev.,* **118,** 2329–2343.

Stamnes, K., S. Tsay, W. Wiscombe, and K. Jayaweera, 1988: Numerically stable algorithm for discrete-ordinate-method radiative transfer in multiple scattering and emitting layered media. *Appl. Opt.,* **27,** 2502–2509.

Stephens, G. L., 1979: Optical properties of eight water cloud types. Division of Atmospheric Physics Tech. Paper 36, CSIRO, Canberra, ACT, Australia, 35 pp.

Stubenrauch, C. J., F. Eddounia, and L. Sauvage, 2005: Cloud heights from TOVS Path-B and LITE observations: Evaluation and seasonal variation of zonal cloud height distributions. *J. Geophys. Res.,* **110,** D19203, doi:10.1029/2004JD005447.

Szejwach, G., 1982: Determination of semi-transparent cirrus cloud temperatures from infrared radiances: Application to Meteosat. *J. Appl. Meteor.,* **21,** 384–393.

Watts, P., C. Mutlow, A. Baran, and A. Zavody, 1998: Study on cloud properties derived from Meteosat Second Generation observations. EUMETSAT Tech. Rep. EUM.ITT.97.181, 344 pp. [Available online at http://www.eumetsat.int/Home/Main/Documentation/Technical_and_Scientific_Documentation/Technical_Memoranda/SP_1124282681564?l=en.]

Weisz, E., J. Li, D. K. Zhou, H.-L. Huang, M. D. Goldberg, and P. Yang, 2007: Cloudy sounding and cloud-top height retrieval from AIRS alone single field-of-view radiance measurements. *Geophys. Res. Lett.,* **34,** L12802, doi:10.1029/2007GL030219.

Zhang, H., and W. P. Menzel, 2002: Improvement in thin cirrus retrievals using an emissivity-adjusted CO_2 slicing algorithm. *J. Geophys. Res.,* **107,** 4327, doi:10.1029/2001JD001037.